2021 IEEE 4th International Conference on Soft Robotics (RoboSoft)
April 12-16, 2021, Yale University, USA

Capacitive sensor measurement rate improves by pre-stretching*

Elze Porte†1, Thomas Sipple†1, Lina Sanchez Botero[1], Dylan Shah[1] and Rebecca Kramer-Bottiglio[1]

2021 IEEE 4th International Conference on Soft Robotics (RoboSoft) | 978-1-7281-7713-7/20/$31.00 ©2021 IEEE | DOI: 10.1109/RoboSoft51838.2021.9479328

***Abstract*— Large-deformation capacitive stretch sensors have proven to be a reliable sensing method for soft robots and wearables. However, the measurement rate at which capacitance is accurately measured is often limited by the relatively high resistance of the conductive composite electrodes. At high measurement frequencies, the measured capacitance underestimates the real capacitance, resulting in inaccurate strain estimation. High measurement rates allow for fast sensor feedback, which is essential for closed loop control of fast moving systems. In this work, we show that the measurement rate of elastic capacitive sensors with conductive composite electrodes can be increased by cyclic pre-stretching of the sensors before each use.**

I. INTRODUCTION

Many soft robots have slow (i.e., sub-Hz) nominal actuation speeds [1], [2]. Recent progress on faster actuation has led to several robots that operate at high actuation frequencies above 10 Hz, including a soft wall-climbing robot [3], and a modular crawling robot using dielectric elastomer actuators [4]. Highly stretchable and fast sensors are required to accurately control these rapidly-actuating robots. Although highly stretchable capacitive sensors are a reliable choice to measure strains in soft robotic systems, with demonstrated closed-loop control [5] and consistent performance over many strain cycles [6], [7], the measurement frequency of these sensors is often limited due to their relatively large size and high electrode resistance [8], [9].

Strain can be measured from a plate capacitor, because its capacitance increases linearly with strain [6], [7], [8]. The capacitance can be determined from impedance measurements, as described in detail by Tayrich and Anderson [8]. In short, the impedance consists of the resistance R and reactance X of the system, and is measured based on the phase shift between an applied voltage signal and the resulting current signal. The measured reactance can be directly translated into capacitance C by:

$$C = \frac{1}{2\pi f \cdot \mid X \mid} \tag{1}$$

where f is the frequency of the applied voltage signal, also referred to as the excitation frequency. A higher excitation frequency results in a higher measurement rate of the capacitance, and therefore of the strain. For example, our LCR meter outputs capacitance data at a maximum rate of 0.5 Hz at an excitation frequency of 200 Hz, and at approximately 100 Hz at an excitation frequency of 10 kHz.

The capacitance measurement is often based on the lumped-parameter model, which assumes the entire sensor can be represented by a single lumped capacitance and lumped resistance [8], [10], [11]. At high measurement frequencies, the lumped model is no longer an accurate representation of the system [8], [12] because the depth of penetration of the applied voltage reduces with increasing frequency [13]. The lower penetration means that the measured capacitance only represents part of the sensor, resulting in a lower measured capacitance that underestimates the experienced strain [8], [9], [12].

Lowering the electrode resistance is expected to increase the frequency at which capacitance, and thus strain, is accurately measured [8]. Repeated stretching of the sensors may decrease the resistance, as is observed in several highly stretchable capacitive [8], [14] and resistive sensors [15], [16], [17], [18], where conductivity is achieved by adding carbon or graphite to a non-conductive matrix. Explanations given for the resistance decrease are hysteresis effects [17], [14], sample slipping from the testing clamps [18], and the creation of new conductive paths with stretch [8].

The aim of this paper is to develop a method that increases the measurement rate of capacitive stretch sensors with conductive composite electrodes. We use cyclic stretching of the sensors to reduce the resistance in the sensor electrodes, which allows for higher measurement rates. We investigate changes in the electrode layers from the stretching process by scanning electron microscope (SEM) imaging, and study the effects of the used strain rate and strain value on the cyclic pre-stretching process. This work contributes to the accurate control of fast actuating soft robotic systems.

II. MATERIALS AND METHODS

A. Sensor fabrication

Sensors were fabricated similar to the method reported by White et al. [6]. In summary, the capacitive sensors consist of two silicone-based electrodes with expanded intercalated graphite (EIG) as conductive filler, separated by a silicone dielectric layer. EIG was prepared by heating expandable graphite flakes (Sigma Aldrich) to 800 °C and subsequent sonication in cyclohexane for 1 h at 70% (Q500 1/2" tip, Qsonica). The EIG-cyclohexane mixture was sieved through a 212 μm mesh and boiled down to achieve approximately 3 wt% EIG. The mixture was manually stirred into DragonSkin10 (Smooth-on, Inc.) at a ratio that achieves 10 wt% EIG after evaporation of the solvent during curing. The EIG-silicone composite was rod-coated on a PET substrate and

*This work was supported by a NASA Small Business Technology Transfer grant (80NSSC17C0030).

† Authors contributed equally to this work

[1]School of Engineering and Applied Sciences, Yale University, New Haven, CT, USA email:{elze.porte, thomas.sipple, lina.sanchez-botero, dylan.shah, rebecca.kramer}@yale.edu

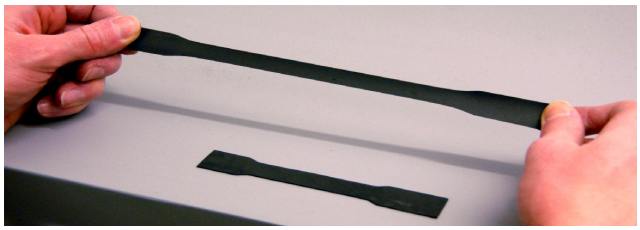

Fig. 1. The elastic capacitive sensors, comprising expanded intercalated graphite-based conductive composite electrodes.

left to cure completely. DragonSkin 10 was rod coated on top of the EIG-silicone layer, and folded onto itself just before full curing to create the 3-layered structure with two electrodes separated by the dielectric. The sensor thickness is approximately 1 mm. Sensors were laser-cut (Universal Laser Systems VLS 2.30, 30 W) to have a rectangular initial active area of 9.8 x 1 cm. Figure 1 shows a picture of the sensors.

B. Cyclic stretching setup

Pre-stretching experiments were carried out using a custom cyclic tester. A detailed description of the tester is captured in Appendix A. In short, the rotational motion of a motor is transmitted to a linear slider to which the sensor is connected, resulting in a fast strain system that is capable of performing hundreds of strain cycles within a couple of minutes. The stretch length of the sensors is controlled by the transmission settings in the hardware. A small pre-strain of approximately 8 mm was applied to all sensors to remove slack in the sensors at 0% strain during testing.

During the standard pre-stretching procedure, sensors were cycled at least 500 times to a maximum deformation of 80 mm at a rate of 60 rpm, resulting in a maximum strain of approximately 75% at a strain rate of 150%/s. The cyclic testing was interrupted at regular intervals to record data while the sensor was stationary at 0 and 75% strain. The effect of strain rate was investigated by performing additional tests at 30 and 90 rpm, and the effect of maximum strain was investigated by increasing the maximum deformation to 150 mm (140% strain) at 32 rpm to ensure a similar strain rate (150%/s) as in the standard tests.

An LCR meter (Keysight E4980A/AL) was used to measure capacitance and resistance of the sensors, using its frequency sweep function. A frequency sweep goes through a series of increasing excitation frequencies, and records the capacitance and resistance for each frequency. Measurements were performed while the sensor was stationary at 0% and 75% strain, regardless of the maximum strain applied in the pre-stretching procedure.

C. Morphology of sensors

The surface morphology of the EIG electrodes was characterized using an SEM (Hitachi SU-70) under an accelerated voltage of 2 kV. All samples were sputter coated with iridium before observation. Samples for SEM characterization were laser-cut from the active area of the sensors.

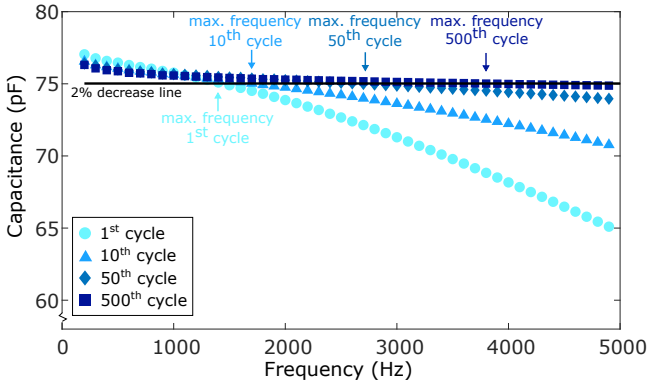

Fig. 2. Representative example of the measured capacitance at 75% strain for the first, 10^{th}, 50^{th}, and 500^{th} strain cycle. The black line indicates the approximate 2% capacitance drop from the measured capacitance at 200 Hz. For clarity, a single 2% decrease line is shown, although in the rest of our reported results the 2% decrease was established from the capacitance at 200 Hz for each measured cycle.

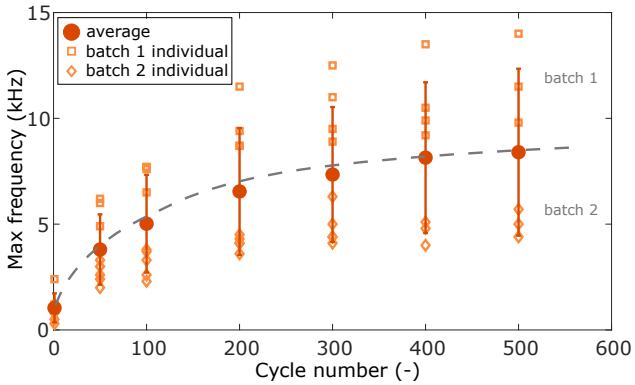

Fig. 3. Average maximum frequency at 75% strain up to 500 cycles with error bars indicating the standard deviation (n = 6-9 after removal of outliers, with data points considered outliers when the sensor was accidentally shorted during the measurement). Individual measurements were included to show divide between sensor batches (n = 2-4 per batch). Dashed gray line was added to guide the reader.

III. RESULTS AND DISCUSSION

A. Characterizing maximum measurement frequency

Repeated stretching of the sensors to 75% strain was performed to increase the maximum excitation frequency at which capacitance was accurately measured. In this paper, we defined the maximum excitation frequency as the frequency at which the measured capacitance at 75% strain fell more than 2% from the capacitance measurement at the lowest tested frequency (200 Hz). For our sensors, this capacitance reduction corresponds to a strain measurement error of less than 5%, which was set as an arbitrary acceptable error. Measured at 200 Hz, the average capacitance change between 0% and 75% strain was 35 pF, and the deviation between capacitance measurements taken at 7 intervals over 500 pre-stretching cycles was less than 1 pF for all tested sensors. The capacitance of the sensors has previously been shown to increase linearly with strain [5], [6].

Fig. 2 shows the measured capacitance at 75% strain up to an excitation frequency of 5000 Hz for a representative sensor sample, including the line that indicates the

2% reduction. The decreasing capacitance with increasing excitation frequency means that the measured capacitance does not represent the actual capacitance at high frequencies for all cycle numbers. The maximum frequency at which the capacitance is accurately measured, where the measured capacitance crosses the 2% decrease line, shifts to higher frequencies with increasing strain cycles.

The maximum frequency increases consistently with the number of cycles across all tested samples (Fig. 3). The average improvement after 500 cycles was approximately 800%, with the largest increase observed within the first 200 cycles (approx. 600%). The improvement between 400-500 cycles was only 3%, so minimal further improvements are expected at higher cycles. Additional measurements after 1000 cycles for five samples only showed an average 6% increase between 500-1000 cycles, confirming the minimal improvement at higher cycles. We do not expect the pre-stretching procedure to have a meaningful effect on the sensor's lifetime, since we have previously tested our sensors up to 100.000 cycles without failure [6].

The relatively large deviation of the average maximum frequency is thought to relate to batch variations. Although the batch sizes are too small to assign statistical significance to the data, the individual sample measurements shown in Fig. 3 indicate that samples can be grouped together in their manufacturing batch with maximum frequencies above (batch 1) and below average (batch 2). Although the manufacturing process was identical between batches, random differences may exist in the thickness of the coated layers, EIG particle size, and EIG concentration in the electrodes. These parameters can affect the conductivity of the electrodes [6], and thus affect the signal penetration depth [8], [13]. The general trend regarding the increased maximum frequency with increasing number of strain cycles can be expected regardless of specific sample characteristics, since similar trends were observed for all samples (Fig. 3).

Dynamic stretching of the sensors was essential to achieve the large increase in maximum frequency. Prolonged static stretching of the sensors did not result in the same improvement. Sensors that were cycled repeatedly (400 cycles at 60 rpm) increased their maximum frequency by an average of 680%, while sensors that were stretched to 75% and held for the same time period (6.7 minutes) showed a maximum increase of only 30%. This suggests that stress-relaxation of the silicone matrix has a minimal effect on maximum frequency, and dynamic stretching is required to use pre-stretching as a method to improve sensor performance.

The maximum frequency increase after pre-stretching the sensors is not a permanent change in the sensor's properties. In a separate test, an average reduction from approximately 5 kHz to 2 kHz maximum frequency was observed for three samples that were left to rest (0% strain) for at least 48 h after cyclic testing. Although the 2 kHz value was higher than the original maximum frequency of the new sensors (approximately 1 kHz), subsequent pre-stretching was required to recover the sensor's maximum frequency to its level observed directly after the initial pre-stretching procedure.

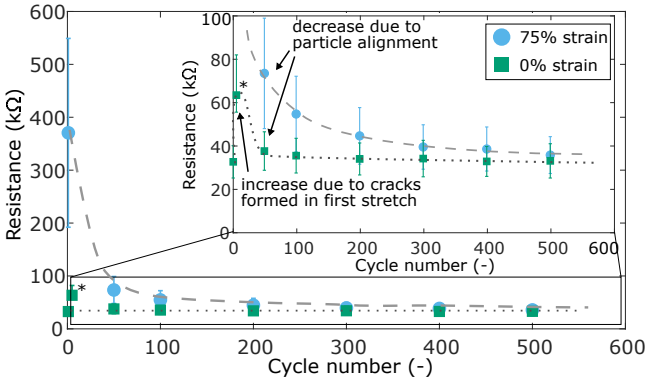

Fig. 4. Average resistance measured at 1 kHz at 0 and 75% strain from the first to the 500^{th} cycle, the error bars indicate the standard deviation (n = 7, (*n = 4, error bars indicate minimum and maximum values)), and the dashed line was added to guide the reader. Inset shows more detail up to 100 kΩ.

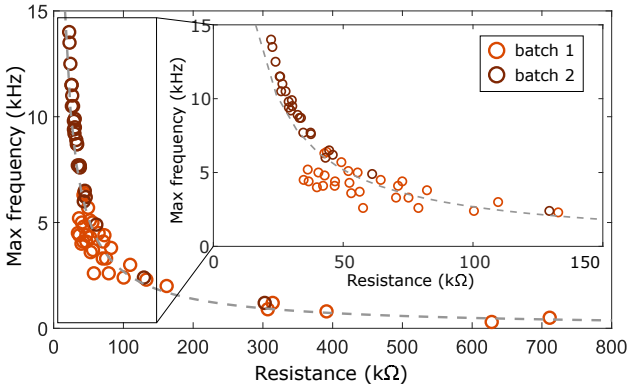

Fig. 5. Relationship between the electrode resistance and maximum excitation frequency. Data points indicate individual measurements, grouped into the two manufacturing batches. Dashed line was added to guide the reader. Inset shows more detail between 0-150 kΩ.

To maximize measurement frequencies, pre-stretching the sensors before each use is therefore recommended.

B. Relating maximum measurement frequency to resistance

The resistance of the sensor electrodes was measured simultaneously with the capacitance to investigate the relationship between electrode resistance and maximum excitation frequency. The resistance of the electrodes was expected to be the determining factor for the penetration depth of the voltage signal, and therefore to be directly related to the maximum frequency. Fig. 4 shows the average resistance response that was measured simultaneously with the capacitance data to determine the maximum frequency in Fig. 3. The resistance was measured at 0% strain in addition to the standard measurements at 75% strain to provide a baseline for the system.

All samples followed the general trend shown in Fig. 4: brand new EIG electrodes exhibit an initial low resistance state (cycle number 0, <40 kΩ), followed by a sudden increase in resistance after the first cycle at both 0 and 75% strain (cycle number 1), and finally a monotonic decrease in resistance with increasing strain cycles (cycle number >1). For all cycle numbers, the electrode resistance at 75% strain

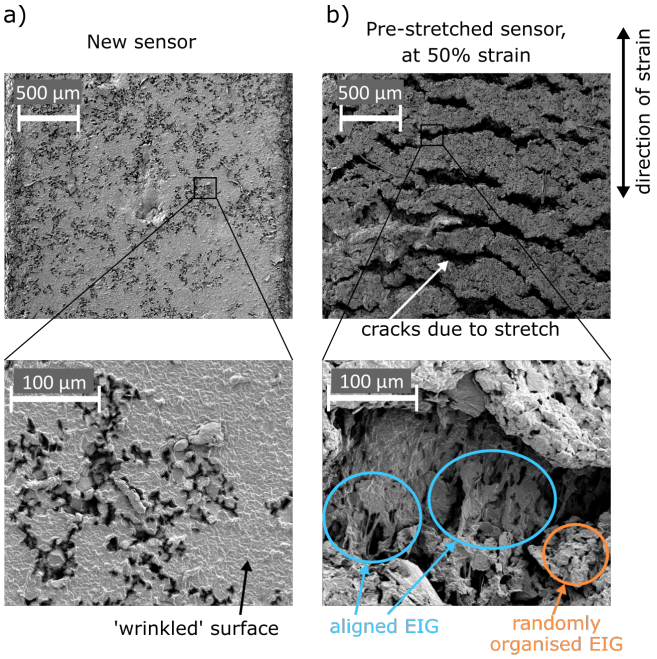

Fig. 6. SEM images of a) new sensor and b) pre-stretched sensor (1000 cycles) under approximately 50% strain.

is higher than at 0% strain. The resistance measured at 75% strain drops rapidly within the first 50 cycles, which is the inverse trend as observed between maximum frequency and cycle number (Fig. 3).

Fig. 5 confirms the relationship between resistance and maximum frequency. The graph shows that the highest maximum frequency was achieved when very low resistance was measured and that a low maximum frequency corresponded to a high resistance. This relationship also confirms the difference between the two manufacturing batches, with batch 2 showing generally low resistance and high maximum frequencies compared to batch 1.

The resistance of the electrodes may be affected by changes in temperature, as observed in resistive sensors [7], [18]. We monitored the temperature of three samples with an infrared thermometer (Lasergrip 800, Etekcity) before, after and half-way through a continuous run of 500 cycles at 90 rpm. The temperature fluctuated within 0.5 °C between measurements, indicating that the sustained strain rate did not lead to an increase in temperature that can explain the changes in the electrode resistance.

To further understand the resistance changes from the dynamic pre-stretching procedure, SEM images of the sensor's electrodes were taken before stretching (Fig. 6a), and while under approximately 50% strain after pre-stretching 1000 cycles to 75% strain (Fig. 6b). Images of the EIG sheets that are used as conductive fillers in the electrodes are shown in Fig. 10 in Appendix B.

The brand new EIG electrode has an interconnected wrinkled surface structure, made up of numerous EIG sheets and silicone resin (Fig. 6a). The isotropic wrinkling structure suggests strong interaction between the EIG sheets in the composite, which leads to a low initial resistance value [19], [20]. The sensors that have been pre-stretched show cracks in the surface perpendicular to the strain direction (Fig. 6b). These cracks form with the first strain of the sensor and are thought to lead to an initial breakdown of the surface conductive network, which can explain the sudden increase in resistance during the first strain cycle. The cracks only appear in the electrodes and do not affect the dielectric layer and the sensor's actual capacitance.

The crack openings in the pre-stretched sensor reveal an inner dense layer of stretched EIG networks, oriented along the direction of strain deformation (Fig. 6b). We hypothesize that the cyclic deformation promotes reordering and alignment of the EIG sheets within the cracks. For uniaxial strain, the sensor becomes compressed transversally, and both forces work in tandem to align and connect the conductive pathways within the cracks, leading to a reduction in electrode resistance which in turn increases the frequency range of the capacitive sensors.

The decrease in resistance under dynamic strain cycles has been reported previously for different carbon based conductive filler/elastomer matrix composites [21], [22], [23], [24], [25]. This behavior has been associated with the formation of additional conductive pathways by the orientation and stacking of conductive aggregates/particles in the composite [22], [23], [24], as well as the breaking [20] and thinning [26] of the polymer matrix induced by shear deformation. All mechanisms improve the contact between the particle filler, resulting in a decrease in the resistance in the conductive composite materials.

The removal of the external force/deformation partially relaxes the system, which increases the resistance of the conductive composite [21]. The relaxation mechanism can explain the observed decrease in the maximum frequency with time when sensors are rested at 0% strain. Re-orientation of the EIG with stretching will happen in subsequent strain cycles, which is in agreement with our observation that electrode resistance increases during rest (0% strain) but can be "recovered" with pre-stretch cycles prior to each use.

C. *Effect of pre-stretching parameters*

Different pre-stretching strain rates and values were tested to investigate their effect on the maximum excitation frequency. No effect of the chosen strain rate was observed, with the tested strain rates ranging from 75 to 225 %/s all showing a very similar increase in the maximum frequency with the number of cycles (Fig. 7). The maximum strain in the pre-stretching process also did not lead to any observable differences. Fig. 8 compares the maximum frequency of sensors that were stretched to 140% strain in the pre-stretching procedure to sensors that were tested in the standard procedure (75% strain, repeated from Fig. 3). All measurements were taken at 75% strain to provide a direct comparison. The graph shows that the maximum frequency of the 140% strain tests fall within the deviation from the sensors pre-stretched to 75% strain. These findings indicate that the number of cycles is the dominant factor to increase

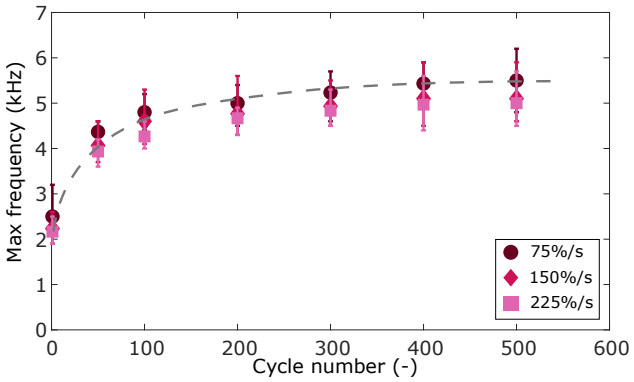

Fig. 7. Average maximum frequency for three different strain rates. Error bars indicate maximum and minimum values (n = 3) and the dashed gray line was added to guide the reader.

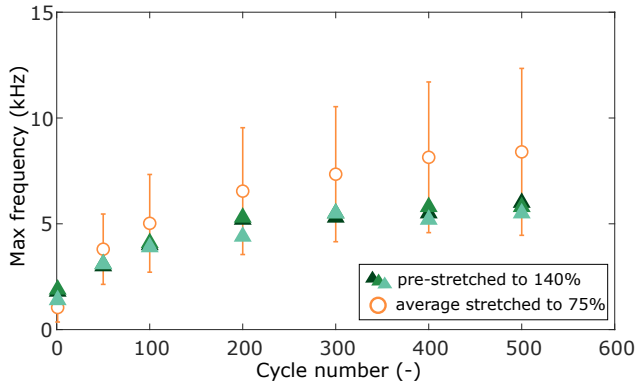

Fig. 8. Maximum frequency up to 500 strain cycles for sensors stretched to 140% strain compared to the average maximum frequency for sensors stretched to 75% strain (repeated from Fig. 1, error bars indicate the standard deviation (n = 6-9)). Maximum frequency was measured at 75% strain for all sensors.

the maximum frequency during the sensor pre-stretching process.

Since we did not observe an effect of the maximum strain value on the maximum frequency, we hypothesize that the sensors may not have to be stretched to their expected maximum strain, and that large improvements may be observed from stretching to lower strain values. Although further work is required to establish a lower limit for the strain value, we hypothesize that alignment of the EIG network may happen when the surface cracks start to clearly appear since the SEM images indicated that EIG sheets align in the direction of strain within the cracks to form a low resistance network. Observing our sensors, we expect this to happen at about 20% strain. We still recommend initially pre-stretching sensors to at least their expected maximum strain to remove any plastic effects that occur from the Mullins effect [27] and initial crack formation.

D. Implications for soft robotic systems

To the best of our knowledge, this is the first study that uses sensor pre-stretching to improve measurement rates. Although a more complicated transmission line model can predict measured lumped capacitance as a function of measuring frequency [8], we are unaware of any methods that can distinguish between true capacitance changes and unintended changes due to high excitation frequencies. Our pre-stretching method provides a practical solution to increase a sensor's maximum excitation frequency and avoid this source of measurement uncertainty.

The pre-stretching method to increase the measurement frequency of the sensors can enable more accurate control of faster moving robots. According to the Nyquist sampling theorem, a signal—such as the motion of a soft robot—can be perfectly reconstructed if the signal is measured at least twice as fast as its highest frequency component. However, noise makes this more complicated in practice, and commonly-accepted best practices suggest that sensing frequencies should be at least 10 times the signal frequency to make sampling rate a negligible source of error, and therefore maximize the controllability of a robot [28]. Although our reported maximum excitation frequencies are in the kHz range, the sensing circuits impose additional reductions in attainable sample rate. For example, our LCR meter could only measure capacitance data at 0.5 Hz with an excitation frequency of 200 Hz, and is limited to a measurement rate of approximately 100 Hz for excitation frequencies above 10 kHz. This means that to measure a robot that exhibits motions with contributing factors above 10 Hz, other measurement techniques are required.

All measurements in the current work were taken with an LCR meter that uses impedance measurements to calculate the capacitance and resistance of the sensors, but the pre-stretching method is also expected to increase the measurement rate using other capacitance-measuring schemes. Other measurement methods include: charging the sensor electrode for a fixed amount of time and measuring the time to decay to a known voltage [6], [29], and charging a sensor for a known amount of time at a constant current and measuring the corresponding maximum attained voltage [30]. The charging times of the sensor will decrease with decreasing resistance, resulting in faster measurement rates for both methods.

Resistive sensors may provide a higher sensing rate compared to capacitive sensors because they do not require charging of the dielectric. Resistive sensors, however, can have other drawbacks. First, the resistance of particle filled sensors can change with the number of strain cycles [15], [16], [17], [18], as we also observe in the resistance measurements of the electrodes in the current work. Second, most resistive sensors have a nonlinear resistance response to strain [7], [18], [31], [32], [33], which complicates calibration of the sensors. It is well documented that capacitive sensors have a linear capacitance response to strain [6], [7], [8], [18]. Third, resistive sensors generally show stronger viscoelastic effects than capacitive sensors, such as hysteresis [7], [18], [31] and overshoot behaviour [18], [33]. The use of capacitive sensors has many benefits, and the pre-stretching method reduces the drawbacks on sensing frequency.

In our recent work, we compared capacitive sensors that used a graphite conductive silicone composite to a multiphase composite (MPC) of eutectic gallium-indium (eGaIn), silicone, and graphite [34]. The low resistance

of the MPC sensors allowed their capacitance to be measured by a circuit with a time constant on the order of microseconds [35], whereas our custom circuit to measure the EIG based sensors operates with a time constant on the order of milliseconds [6], [29]. However, the MPC sensors' performance comes with drawbacks: increased expense, a narrower operating temperature range (eGaIn solidifies below 15°C), and an increased likelihood of short-circuiting when eGaIn leaks out of the sensors due to cuts or manufacturing imperfections. The current pre-stretching method provides a solution to cheap, reliable, and fast sensing.

IV. CONCLUSIONS

The maximum measurement frequency was investigated during cyclic stretching of capacitive stretch sensors. Two main conclusions were drawn. First, the maximum frequency was increased by reducing the electrode resistance, which was achieved by repeatedly stretching the sensors before use. Second, the most important pre-stretching parameter was the number of strain cycles. No effect of strain rate and strain value was observed. Collectively, these results point to the potential of pre-stretching conductive composite dielectric elastomer sensors prior to use to achieve optimal sensor readings at high sensing frequencies.

APPENDIX

A. Custom cyclic tester details

The setup consists of a motor, connection disk, connection arm, and linear guidance slider (Fig. 9). The motor directly drives to connection disk, and motion is transferred to the linear guidance slider by the connection arm between the slider and disk. The further the connecting arm is placed towards the outside of the disk, the larger the maximum strain. One end of the sensor was kept stationary, while the other end was mounted on the slider. Each cycle of the motor results in one strain cycle of a sensor. The motor is controlled by an Arduino Uno and Cytron motor shield, and powered by a 12 volt power supply. The motor speed is controlled by a closed loop system utilizing a shaft encoder to ensure that the chosen rpm is maintained throughout the trial.

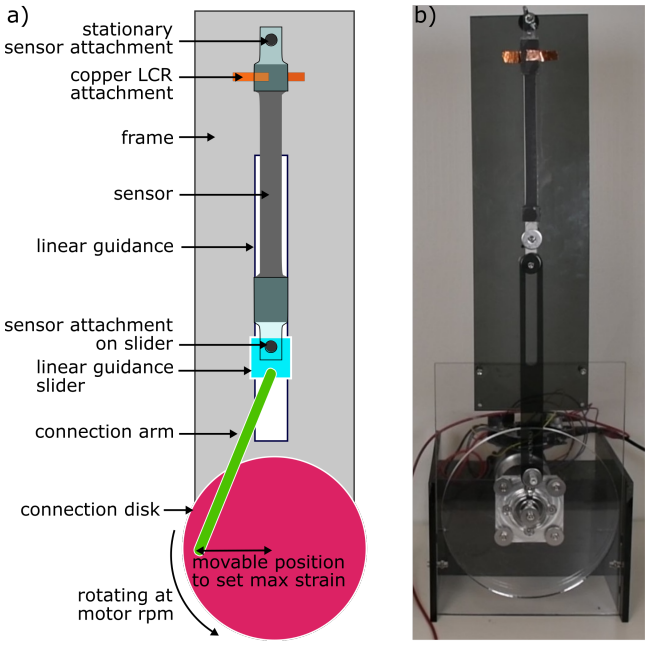

Fig. 9. Custom cyclic testing setup: a) schematic; b) picture.

B. EIG morphology

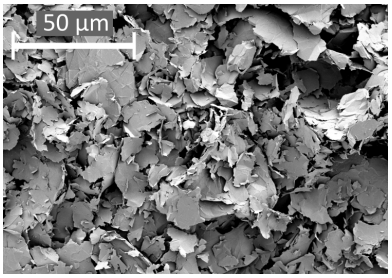

Fig. 10. SEM image of EIG sheets.

ACKNOWLEDGMENT

E.P., T.S., and R.K.B. thank our collaborators at Otherlab: Karen Robinson, Tim Duggan, Conor O'Brien, and Jim McBride for valuable discussions regarding the applications of this work.

REFERENCES

[1] S. Seok, C. D. Onal, K. J. Cho, R. J. Wood, D. Rus, and S. Kim, "Meshworm: A peristaltic soft robot with antagonistic nickel titanium coil actuators," *IEEE/ASME Transactions on Mechatronics*, vol. 18, no. 5, pp. 1485–1497, 2013.

[2] R. F. Shepherd, F. Ilievski, W. Choi, S. A. Morin, A. A. Stokes, A. D. Mazzeo, X. Chen, M. Wang, and G. M. Whitesides, "Multigait soft robot," *Proceedings of the National Academy of Sciences*, vol. 108, pp. 20400–20403, Dec. 2011.

[3] G. Gu, J. Zou, R. Zhao, X. Zhao, and X. Zhu, "Soft wall-climbing robots," *Science Robotics*, vol. 3, p. eaat2874, Dec. 2018.

[4] M. Duduta, D. R. Clarke, and R. J. Wood, "A high speed soft robot based on dielectric elastomer actuators," in *2017 IEEE International Conference on Robotics and Automation (ICRA)*, pp. 4346–4351, May 2017.

[5] M. C. S. Yuen, T. R. Lear, H. Tonoyan, M. Telleria, and R. Kramer-Bottiglio, "Toward closed-loop control of pneumatic grippers during pack-and-deploy operations," *IEEE Robotics and Automation Letters*, vol. 3, no. 3, pp. 1402–1409, 2018.

[6] E. L. White, M. C. Yuen, J. C. Case, and R. K. Kramer, "Low-cost, facile, and scalable manufacturing of capacitive sensors for soft systems," *Advanced Materials Technologies*, vol. 2, no. 9, p. 1700072, 2017.

[7] J. Shintake, E. Piskarev, S. H. Jeong, and D. Floreano, "Ultrastretchable strain sensors using carbon black-filled elastomer composites and comparison of capacitive versus resistive sensors," *Advanced Materials Technologies*, vol. 3, no. 3, p. 1700284, 2018.

[8] A. Tairych and I. A. Anderson, "Capacitive stretch sensing for robotic skins," *Soft Robotics*, vol. 6, no. 3, pp. 389–398, 2019.

[9] D. Xu, S. Michel, T. McKay, B. O'Brien, T. Gisby, and I. Anderson, "Sensing frequency design for capacitance feedback of dielectric elastomers," *Sensors and Actuators, A: Physical*, vol. 232, pp. 195–201, 2015.

[10] G. Rizzello, D. Naso, A. York, and S. Seelecke, "A self-sensing approach for dielectric elastomer actuators based on online estimation algorithms," *IEEE/ASME Transactions on Mechatronics*, vol. 22, no. 2, pp. 728–738, 2017.

[11] T. Hoffstadt, M. Griese, and J. Maas, "Online identification algorithms for integrated dielectric electroactive polymer sensors and self-sensing concepts," *Smart Materials and Structures*, vol. 23, no. 10, 2014.

[12] M. P. Tiggelman, K. Reimann, J. Liu, M. Klee, W. Keur, R. Mauczock, J. Schmitz, and R. J. Hueting, "Identifying dielectric and resistive electrode losses in high-density capacitors at radio frequencies," *IEEE International Conference on Microelectronic Test Structures*, pp. 190–195, 2008.

[13] C. Graf and J. Maas, "A model of the electrodynamic field distribution for optimized electrode design for dielectric electroactive polymer transducers," *Smart Materials and Structures*, vol. 21, no. 9, 2012.

[14] D. J. Cohen, D. Mitra, K. Peterson, and M. M. Maharbiz, "A highly elastic, capacitive strain gauge based on percolating nanotube networks," *Nano Letters*, vol. 12, no. 4, pp. 1821–1825, 2012.

[15] Z. Yang, Y. Pang, X. L. Han, Y. Yang, Y. Yang, J. Ling, M. Jian, Y. Zhang, and T. L. Ren, "Graphene textile strain sensor with negative resistance variation for human motion detection," *ACS Nano*, vol. 12, no. 9, pp. 9134–9141, 2018.

[16] V. Kumar, M. N. Alam, A. Manikkavel, J. Choi, and D. J. Lee, "Investigation of silicone rubber composites reinforced with carbon nanotube, nanographite, their hybrid, and applications for flexible devices," *Journal of Vinyl and Additive Technology*, no. July, pp. 1–10, 2020.

[17] Y. Pang, Z. Yang, X. Han, J. Jian, Y. Li, X. Wang, Y. Qiao, Y. Yang, and T. L. Ren, "Multifunctional mechanical sensors for versatile physiological signal detection," *ACS Applied Materials and Interfaces*, vol. 10, no. 50, pp. 44173–44182, 2018.

[18] M. Amjadi, Y. J. Yoon, and I. Park, "Ultra-stretchable and skin-mountable strain sensors using carbon nanotubes-Ecoflex nanocomposites," *Nanotechnology*, vol. 26, no. 37, 2015.

[19] H. Liu, Y. Li, K. Dai, G. Zheng, C. Liu, C. Shen, X. Yan, J. Guo, and Z. Guo, "Electrically conductive thermoplastic elastomer nanocomposites at ultralow graphene loading levels for strain sensor applications," *J. Mater. Chem. C*, vol. 4, pp. 157–166, 2016.

[20] L. Flandin, A. Chang, S. Nazarenko, A. Hiltner, and E. Baer, "Effect of strain on the properties of an ethylene–octene elastomer with conductive carbon fillers," *Journal of Applied Polymer Science*, vol. 76, no. 6, pp. 894–905, 2000.

[21] L. Flandin, A. Hiltner, and E. Baer, "Interrelationships between electrical and mechanical properties of a carbon black-filled ethylene–octene elastomer," *Polymer*, vol. 42, no. 2, pp. 827 – 838, 2001.

[22] K. Yamaguchi, J. J. C. Busfield, and A. G. Thomas, "Electrical and mechanical behavior of filled elastomers. i. the effect of strain," *Journal of Polymer Science Part B: Polymer Physics*, vol. 41, no. 17, pp. 2079–2089, 2003.

[23] L. Lin, S. Liu, S. Fu, S. Zhang, H. Deng, and Q. Fu, "Fabrication of highly stretchable conductors via morphological control of carbon nanotube network," *Small*, vol. 9, no. 21, pp. 3620–3629, 2013.

[24] H. Deng, M. Ji, D. Yan, S. Fu, L. Duan, M. Zhang, and Q. Fu, "Towards tunable resistivity–strain behavior through construction of oriented and selectively distributed conductive networks in conductive polymer composites," *J. Mater. Chem. A*, vol. 2, pp. 10048–10058, 2014.

[25] H. Yazdani, K. Hatami, E. Khosravi, K. Harper, and B. P. Grady, "Strain-sensitive conductivity of carbon black-filled pvc composites subjected to cyclic loading," *Carbon*, vol. 79, pp. 393 – 405, 2014.

[26] S. Shenogin, L. Ferguson, and A. K. Roy, "The effect of contact resistance on electrical conductivity in filled elastomer materials," *Polymer*, vol. 198, p. 122502, 2020.

[27] J. Diani, B. Fayolle, and P. Gilormini, "A review on the Mullins effect," *European Polymer Journal*, vol. 45, no. 3, pp. 601–612, 2009.

[28] Y. Duan and H. Jin, "Digital controller design for switchmode power converters," in *APEC '99. Fourteenth Annual Applied Power Electronics Conference and Exposition. 1999 Conference Proceedings (Cat. No.99CH36285)*, vol. 2, pp. 967–973 vol.2, Mar. 1999.

[29] E. L. White, J. C. Case, and R. Kramer-Bottiglio, "A Soft Parallel Kinematic Mechanism," *Soft robotics*, vol. 5, no. 1, pp. 36–53, 2018.

[30] M. D. Bartlett, E. J. Markvicka, and C. Majidi, "Rapid Fabrication of Soft, Multilayered Electronics for Wearable Biomonitoring," *Advanced Functional Materials*, vol. 26, pp. 8496–8504, Dec. 2016.

[31] S. Y. Kim, Y. Choo, R. A. Bilodeau, M. C. Yuen, G. Kaufman, D. S. Shah, C. O. Osuji, and R. Kramer-Bottiglio, "Sustainable manufacturing of sensors onto soft systems using self-coagulating conductive Pickering emulsions," *Science Robotics*, vol. 5, no. 39, p. eaay3604, 2020.

[32] S. Xu, D. M. Vogt, W. H. Hsu, J. Osborne, T. Walsh, J. R. Foster, S. K. Sullivan, V. C. Smith, A. W. Rousing, E. C. Goldfield, and R. J. Wood, "Biocompatible Soft Fluidic Strain and Force Sensors for Wearable Devices," *Advanced Functional Materials*, vol. 29, no. 7, pp. 1–14, 2019.

[33] P. Lugoda, J. C. Costa, L. A. Garcia-Garcia, A. Pouryazdan, Z. Jocys, F. Spina, J. Salvage, D. Roggen, and N. Münzenrieder, "Coco Stretch: Strain Sensors Based on Natural Coconut Oil and Carbon Black Filled Elastomers," *Advanced Materials Technologies*, vol. 2000780, pp. 1–9, 2020.

[34] R. A. Bilodeau, A. M. Nasab, D. S. Shah, and R. Kramer-Bottiglio, "Uniform conductivity in stretchable silicones via multiphase inclusions," *Soft Matter*, vol. 16, pp. 5827–5839, July 2020. Publisher: The Royal Society of Chemistry.

[35] Freescale Semiconductor, "MPR121 Capacitive Touch Sensor Controller." https://www.digikey.com/htmldatasheets/production/1654880/0/0/1/MPR121.pdf, Feb. 2013. Accessed: 2020-11-06.